Astronomical Data Analysis Software and Systems X
ASP Conference Series, Vol. 238, 2001
F. R. Harnden Jr., F. A. Primini, and H. E. Payne, eds.

Kalman Filtering in Chandra Aspect Determination

Roger Hain, Thomas L. Aldcroft, Robert A. Cameron, Mark Cresitello-Dittmar, Margarita Karovska

Harvard-Smithsonian Center for Astrophysics, 60 Garden St., Cambridge, MA 02138

Abstract. The ability of the Chandra X-ray Observatory to achieve unprecedented image resolution is due, in part, to its ability to accurately reconstruct the spacecraft attitude history. This is done with a Kalman filter and Rauch-Tung-Striebel (RTS) smoother, which are key components of the overall aspect solution software. The Kalman filter/RTS smoother work by combining data from star position measurements, which are accurate over the long term but individually noisy, and spacecraft rate information from on-board gyroscopes, which are very accurate over the short-term, but are subject to drifts in the bias rate over longer time scales. The strengths of these two measurement sources are complementary. The gyro rate data minimizes the effects of noise from the star measurements, and the long-term accuracy of the star data provides a high-fidelity estimate of the gyro bias drift. Analysis of flight data, through comparison of observed guide star position with expected position and examination of the reconstructed X-ray image point spread function, supports the conclusion that performance goals (1.0 arcsecond mean aspect error, 0.5 arcsecond aspect error spread diameter) were met.

1. Application of Kalman Filtering in Chandra

The schematic shown in Figure 1 illustrates the basic flow of the Kalman filter design for Chandra aspect determination (Gelb 1974, TRW Memorandum 1996). The main purpose of the filter is to derive an accurate estimate of the spacecraft angular position, or attitude, at any time. Together with fiducial light data for estimating spacecraft flex, this attitude estimate is used to accurately determine the source in the celestial sphere of X-rays detected by the science instruments. Details of the hardware, ground software, and flight performance are given in Aldcroft et al. (2000) and Cameron et al. (2000).

The filter estimates 3-axis error in current attitude estimate and 3-axis gyroscope drift rate, resulting in six estimated quantities referred to as the filter "state." The schematic illustrates the basic flow of the filter. Beginning with an initial state estimate, and initial statistics which characterize how well the state estimates are known (the "covariance"), the filter iterates through two steps.

First, as shown in the upper left box, gyro data are received. The state estimate of gyro bias is subtracted from the raw gyro data, and the spacecraft attitude is updated according to the angular motion derived from the corrected

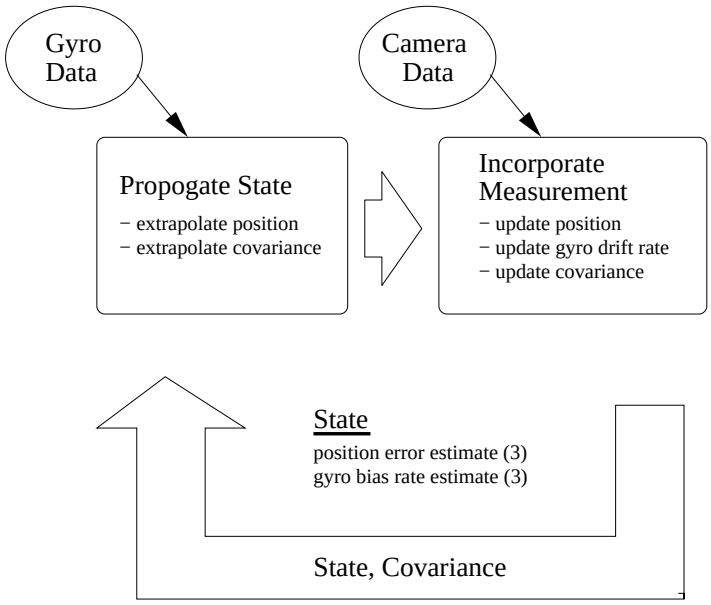

Figure 1. Chandra Aspect Kalman Filter Schematic.

gyro data. The error statistics associated with the state are also updated, since both uncertainty in gyro bias and attitude errors due to rate uncertainty grow over time. In this way, state and attitude estimates are maintained and propagated forward in time until a star camera measurement is available.

The second step is shown in the upper right box. A measurement (the location of a guide star) is received from the aspect camera and incorporated into the filter's state estimates and error statistics. The filter mathematically compares the new attitude estimate based on the current measurement with the expected attitude from the prior propagation step. Using the expected attitude error and the expected measurement error (the star camera noise), new estimates of attitude error and gyro bias drift are calculated. After incorporating these new data, the error statistics are updated to reflect more accurate attitude knowledge, and the cycle begins again.

The four charts in Figure 2 illustrate the aspect pipeline Kalman filter's behavior over time using simulated data. In the upper left graph, the solid line shows the actual pitch estimate error for a 500 second nominal dither observation. The dashed lines represent the root mean square (RMS) value of the covariance for pitch error (i.e., the filter's own estimate of the 1-σ uncertainty in pitch estimate). Note that in this plot and the yaw plot below it, the error in each axis quickly converges to a steady state value. The two charts shown on the right demonstrate the improvement in pitch and yaw estimate error with the addition of a smoothing algorithm. The use of a smoother is possible since the processing is done post-facto. The smoother allows better overall estimates and much improved performance in the very early part of the data. The smoother accomplishes this by utilizing state and measurement data from the entire time period to improve the estimate at each point in time. The filter alone is not able to use future data to produce estimates.

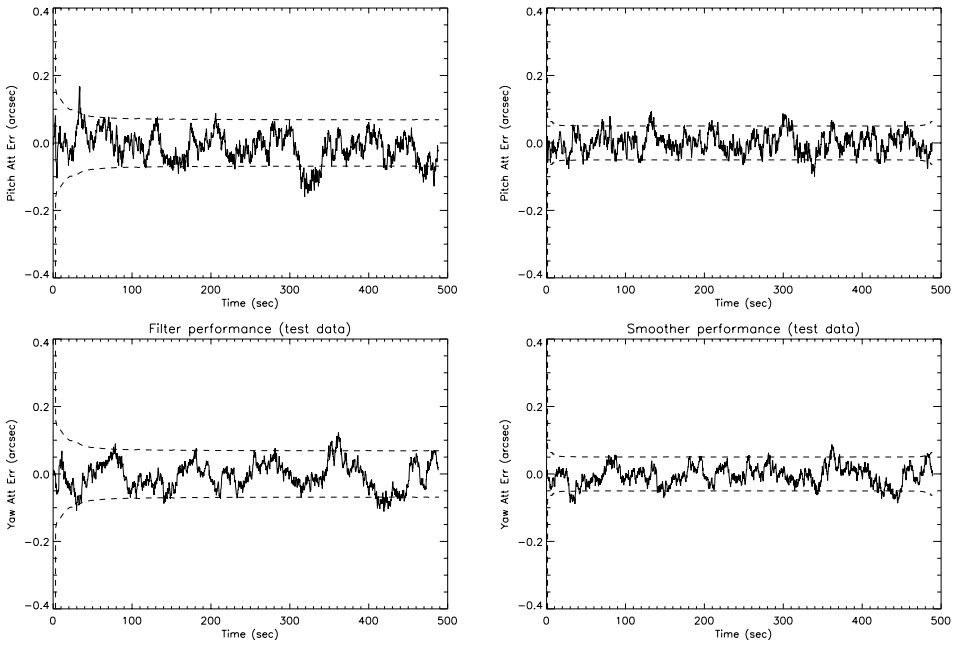

Figure 2. Sample filter and smoother results.

2. Measuring Aspect Performance

To quantify overall aspect quality a 50,000 second observation was examined. An X-ray point source was identified in this observation, and a circular region around the point source with a radius of approximately 2 arcseconds was isolated. Aspect corrected coordinates for the source photons were then examined in a coordinate system aligned with the spacecraft reference frame. This coordinate system is chosen since residual aspect errors are expected to be most visible near the dither frequency, and such errors are more clearly visible as a single frequency oscillation in these coordinates. The corrected sky coordinates did not show any visible oscillations. The power spectrum of photon positions also showed no peaks above the background noise. However, the amount of noise due to photon counting statistics is large compared to the expected aspect oscillations. To improve the SNR of any signal at the dither frequency, the data were phase modulated at the dither frequency. This was done by resetting event times to "time mod(dither period)."

The phase modulated data are shown in Figure 3. Time only goes from 0 to the dither period, and events later than an integer number of dither periods are wrapped back to start at time 0 again. In this way, any residual aspect error at the dither frequency is preserved in the data, but random noise is reduced by averaging. The top charts show phase modulated data for the sky coordinates transformed to the spacecraft X axis (left) and Y axis (right).

The two lower charts show the same data binned on 50 second intervals, with the intention of reducing noise. If no residual oscillation were present, the values of the binned data points would become smaller as the bin size becomes larger, without showing any noticeable constant offset. If, on the other hand, a clear

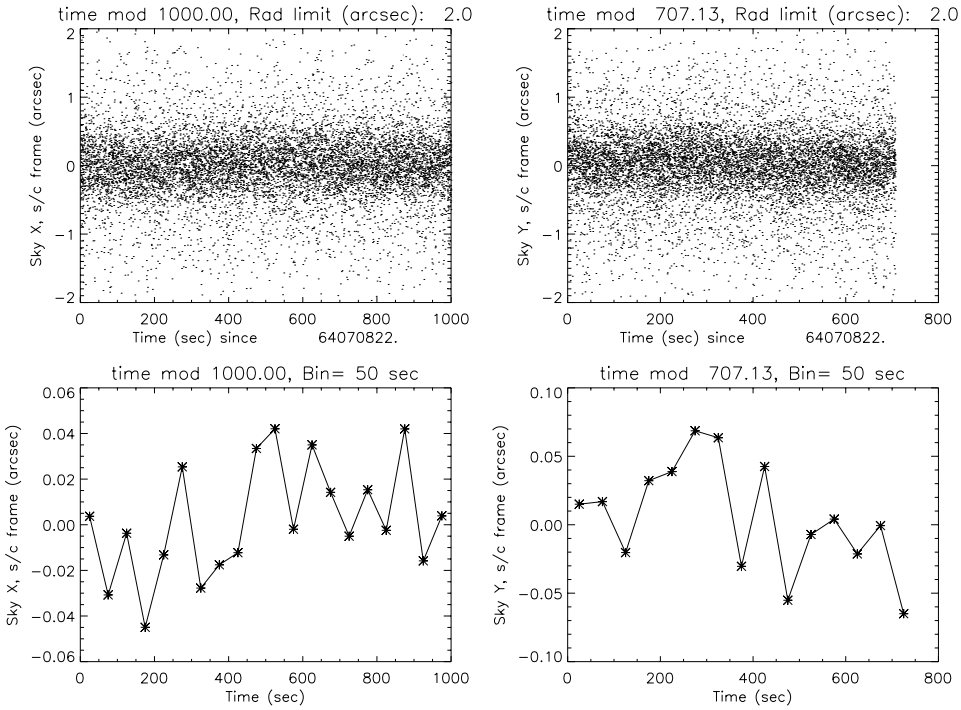

Figure 3. Aspect error in event reconstruction.

signal were present, this should become apparent in the structure of the binned data points. Although even the worst case binned data point is very small (less than 0.08 arcseconds), some slight evidence of a residual signal may be present in the Y coordinate charts. The binned data show a disproportionate number of positive data points in the first half of the dither interval, and a disproportionate number of negative data points in the second half. Note, however, that even if this error is entirely due to aspect error and not noise, the worst case still compares very favorably with the 0.5 arcsecond spread diameter requirement.

This project is supported by the Chandra X-ray Center under NASA contract NAS8-39073.

References

Gelb, A. 1974, Applied Optimal Estimation (Cambridge, MA: MIT Press)

Aldcroft, T. L., Karovska, M., Cresitello-Dittmar, M. L., Cameron, R. A., & Markevitch, M. L. 2000, Proc. SPIE, 4012, 650

Cameron, R. A., Aldcroft, T. L., Podgorski, W. A., Freeman, M. D., & Shirer, J. J. 2000, Proc. SPIE, 4012, 658

TRW Memorandum, AXAF Attitude and Aspect Determination, 52100.300.087 TRW-SE11K, January 11, 1996